Numerical solution of the Smoluchowski kinetic equation and asymptotics of the distribution function

1995 J. Phys. A: Math. Gen. 28 2025

(http://iopscience.iop.org/0305-4470/28/7/022)

J. Phys. A: Math. Gen. 28 (1995) 2025–2039. Printed in the UK

Numerical solution of the Smoluchowski kinetic equation and asymptotics of the distribution function

D S Krivitsky

Institute of Radio Astronomy of the Ukrainian National Academy of Sciences, Krasnoznamennaya Street, 4, Kharkov, 310002, Ukraine

Received 27 July 1994, in final form 9 November 1994

Abstract. We obtain the numerical solution of the Smoluchowski kinetic equation for model kernels $U(M_1, M_2) \propto (M_1 + M_2)^\lambda$ and $U(M_1, M_2) \propto (M_1 M_2)^{\lambda/2}$, $0 < \lambda \leqslant 2$. We show that the behaviour of the solution for the kernel $U \propto (M_1 + M_2)^\lambda$ at $0 < \lambda \leqslant 1$ and $U \propto (M_1 M_2)^{\lambda/2}$ at $0 < \lambda \leqslant 2$ becomes self-similar after some time. The shape of the scaling function is analysed; in particular, a simple approximate expression for it at $U \propto (M_1 + M_2)^\lambda$ is found. An interesting result is obtained for $U \propto (M_1 M_2)^{\lambda/2}$, $0 < \lambda < 1$: the asymptotic behaviour of the scaling function proved to be non-power. We develop the procedure for determining t_{cr}, the critical indices and the exponent of the power-law asymptotics of the Smoluchowski equation solution. The concrete values of these quantities for the model kernels are obtained. The stability conditions of the algorithm for numerical solving are analysed. The possibilities afforded by numerical solution for investigation of the Smoluchowski equation are discussed.

1. Introduction

The Smoluchowski kinetic equation†

$$\frac{\partial f(M,t)}{\partial t} = \int_0^M U(M_1, M - M_1) f(M_1, t) f(M - M_1, t)\, \mathrm{d}M_1 - 2 f(M,t) \int_0^\infty U(M_1, M) f(M_1, t)\, \mathrm{d}M_1 \tag{1}$$

which describes the evolution of the mass distribution function $f(M,t)$ of particles due to coalescence, is used in different branches of physics: geophysics (coalescence of water drops in clouds) [1], physical chemistry (coagulation and gel formation) [2], astrophysics (mergers of clouds in interstellar medium, mergers of galaxies) [3, 4].

In particular, the solution of the Smoluchowski equation allows us to obtain the mass distribution function of galaxies formed due to mergers. This, in turn, gives us the possibility of finding the time dependence of the density of quasars as well as their luminosity distribution in the model [5, 6] which relates the activity of galactic nuclei to mergers.

The function $U(M_1, M_2)$, which appears in the equation as a kernel, characterizes the probability of the coalescence of two particles with masses M_1 and M_2. Usually it is

† In this work we use the continuous version of the equation. Note also that in the literature the definition of U often differs from ours by the factor 2. This means that all times in our article differ by the same factor.

0305-4470/95/072025+15$19.50

considered to be a homogeneous function of degree λ, and its asymptotic properties are described by the parameters μ and ν:

$$U(aM_1, aM_2) = a^\lambda U(M_1, M_2)$$

$$U(M_1, M_2) \approx \text{constant } M_1^\nu M_2^\mu \qquad M_1 \gg M_2$$

$$\mu + \nu = \lambda.$$

(In applications of (1) to coagulation there is a physical constraint $\nu \leqslant 1$, but in astrophysics (mergers of galaxies) the case $\nu > 1$ is very important (see $U(M_1, M_2)$ below).)

Exact analytical solutions of the Smoluchowski equation are known only for the three cases: U = constant; $U \propto (M_1 + M_2)$; $U \propto M_1 M_2$; and for some of their linear combinations (see [1,2,7] as reviews, see also original works [8,9]). There are analytical asymptotics for some kernels. These, however, are not known for all kernels and are often based on the hypothesis that the behaviour of the solution is self-similar, which itself requires verification. In this connection, numerical solution of equation (1) is necessary.

In this work we investigate the solution of the Smoluchowski equation for two classes of model kernels: $U \propto (M_1 + M_2)^\lambda$ and $U \propto (M_1 M_2)^{\lambda/2}$, $0 < \lambda \leqslant 2$. There is an exactly solved case, which can be used for a test, in each of the classes: $\lambda = 1$ and $\lambda = 2$ respectively (and the solved case U = constant belongs to both classes). The kernel $U \propto (M_1 + M_2)^\lambda$ with $\lambda = 2$ appears in the simple model [5] for mergers of galaxies at small masses. The probability of merger at large masses in the same model is $U \propto (M_1 + M_2)(M_1^\beta + M_2^\beta)$, $\beta = 0.3$–0.5; this kernel belongs to the same class $\mu = 0$, and its properties are analogous to those of the kernel $U \propto (M_1 + M_2)^\lambda$. The probability of merger, proportional to the product of masses $U \propto M_1 M_2$, is also possible for galaxies under certain conditions [10]. The kernel $U \propto (M_1 M_2)^{\lambda/2}$ also arises in a certain model of aggregation of clusters in dispersed systems [2]. In this work we consider both the case $\lambda > 1$, corresponding to the critical behaviour of the system, and $\lambda \leqslant 1$. The initial distribution is taken in the form

$$f_0(M) = (N_0/M_*) \exp(-M/M_*). \tag{2}$$

The solution of the Smoluchowski equation is known to quickly lose the details of the initial distribution at large masses, if f_0 decreases rapidly ($\leqslant \exp(-kM)$). So, the choice of the initial distributions is not very important.

In section 2 the method we use for solving the Smoluchowski equation is described and the problem of the stability of the algorithm is discussed. In particular, we show that for rapidly growing kernels the required time stepsize decreases with the limit mass $M_{\max}$. In section 3 dependence of the solution on the limit mass $M_{\max}$, for which computations are executed, is investigated. For $U \propto (M_1 + M_2)^\lambda$, $\lambda > 1$ the value of $M_{\max}$ proved to influence strongly the solution; for $\lambda < 1$, as well as for $U \propto (M_1 M_2)^{\lambda/2}$, this influence is weak. In section 4 we explore the cases for which the solution shows self-similar behaviour and the shape of the scaling function. In particular, we show that for $U \propto (M_1 + M_2)^\lambda$, $\lambda < 1$ this function has power-law asymptotics; for $U \propto (M_1 M_2)^{\lambda/2}$, $\lambda < 1$ the asymptotics are non-power and do not coincide with the analytical expression $M^{-(\lambda+1)}$ known before (figures 1(*c*) and 5(*b*) give a very interesting and important result that the asymptotics are non-power). In section 5 the exponents of the power-law intermediate asymptotics of $f(M, t)$, the critical indices for $\lambda > 1$ and the values of t_{cr} are considered. The conclusions are in section 6.

2. Methods for numerical solution of the Smoluchowski equation and their stability

2.1. Solution methods

To solve differential equation (1) we used the second-order Runge–Kutta method. The collision integral on the right-hand side was computed by the trapezoidal formula. In order to obtain the distribution function in a wide mass range, the substitution of variables

$$M \to z = \log_{10}(M + \text{constant})$$

was made in equation (1) (the constant was added in order to avoid expanding the range of integration to $-\infty$). Such a substitution is equivalent to a variable mass stepsize, increasing with M, in numerical integration. Variable stepsize is often used to solve equation (1) numerically (see [11]).

To compute the first term in the collision integral, one has to know the distribution function not only on the points of the grid M_i, but also between them (to find $f(M - M_1)$). We used interpolation by the formula†

$$\ln f(M) \approx \ln f_i + \frac{\ln f_{i+1} - \ln f_i}{M_{i+1} - M_i}(M - M_i) \qquad M_i \leqslant M \leqslant M_{i+1}$$
$$f_i = f(M_i) \qquad f_{i+1} = f(M_{i+1}). \tag{3}$$

In the second term of (1) the infinity in the upper integral limit was replaced by some large, but finite $M_{\max}$. The influence of the finiteness of $M_{\max}$ on the solution is considered in section 3.

To estimate the error in the present method, we compare the numerical solution with the exact one known for $U \propto (M_1 + M_2)$ and $U \propto M_1 M_2$. Results, shown in figure 1(a), exhibit good agreement. Another way to check the error is to use the total mass conservation law, for $t < t_{cr}$ when $\lambda > 1$ and for all t when $\lambda \leqslant 1$. The total mass $\mathcal{M} = \int_0^\infty Mf(M, t)\,dM$ is conserved in our computations with an error ~ 0.3–3%, while the inequality $s(t) \ll M_{\max}$ is realized ($s(t)$ characterizes the position of the coagulation front or the so called 'mean cluster size', see section 4). A slow change (increase) in $\mathcal{M}$ is related mainly to the interpolation error in formula (3); this error decreases rapidly with decrease in the mass stepsize. As $s(t)$ has become of the order of $M_{\max}$, the total mass begins to decrease. This effect is discussed in section 3.

The main part of the calculations was done on a computer with an Intel 386SX processor (20 MHz), CPU time per one kernel (one λ) was from several minutes to several hours, depending on the parameters (pure calculation time, without processing the results and without the time for debugging the program).

2.2. Stability of the numerical solving algorithm

In some cases (for rapidly growing kernels) a strange phenomenon took place. At some time a small distortion appeared on the plot of the distribution function; the function became non-monotonic. Then the distortion grew rapidly and, after a short time, the program failed (e.g. due to overflow or invalid floating point operation). It was found that, in these cases, a very small time stepsize Δt is necessary for the procedure to be stable, and the stepsize needed decreases rapidly with increasing $M_{\max}$. The common condition that Δt must be much less

† This formula is exact for such functions as $f(M) = A\exp(-kM)$.

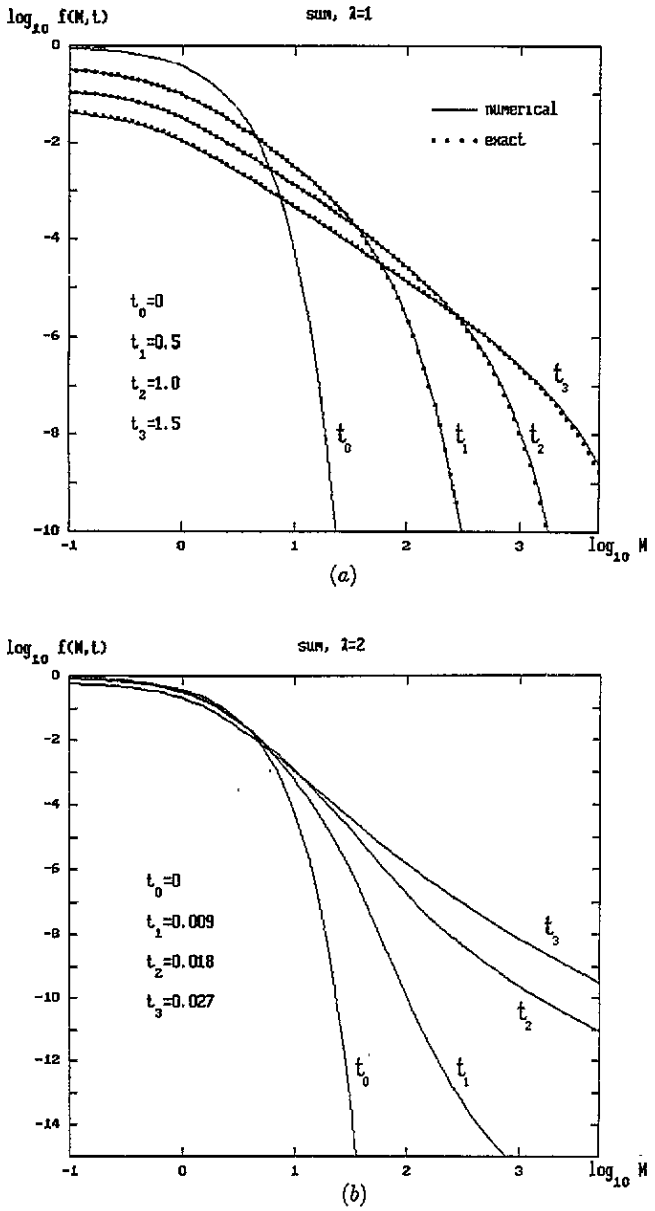

Figure 1. (*a*) The solution of the Smoluchowski equation with $U = c(M_1 + M_2)$ for initial distribution (2). The numerical solution (full curve) shows good agreement with the exact one [1] (small rectangles). At large enough t three mass regions may be distinguished: at $M_* \ll M \ll s(t)$ ($s(t)$ is the position of the coagulation front, see section 4) $f(M) \propto M^{-\alpha}$ (a straight line in logarithmic coordinates); at $M \gtrsim s(t)$ $f(M,t)$ decreases exponentially; at $M \lesssim M_*$ information about the initial distribution is retained. Mass in this and other figures is given in units M_*, time in units $1/(cN_0M_*^{\lambda})$, f in units N_0/M_*. (*b*) The numerical solution for $U = c(M_1 + M_2)^2$. A slowly decreasing distribution tail is formed very early ('instantaneous gelation', [14]); the intermediate asymptotics seems to be non-power-law. (*c*) The numerical solution for $U = c(M_1M_2)^{\lambda/2}$, $\lambda = 0.4$. The intermediate asymptotics at $M_* \ll M \ll s(t)$ are non-power-law and do not agree with the known solution $M^{-(\lambda+1)}$: the corresponding part of the curve in the figure is not straight, as it is for a power function, but convex downward.

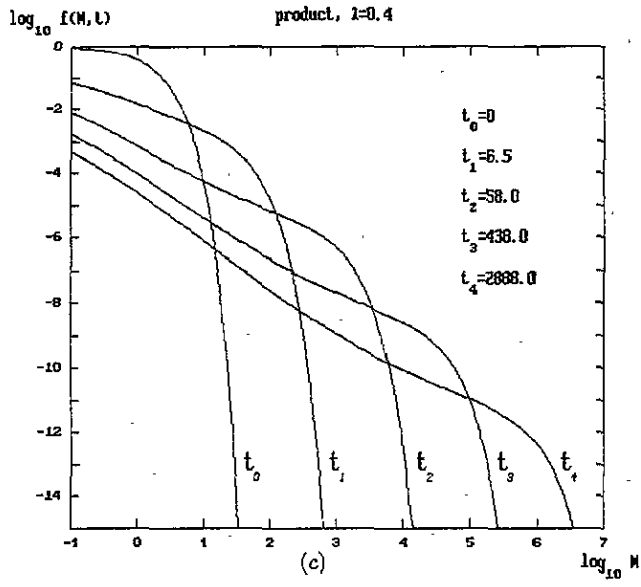

Figure 1. (Continued)

than the typical time for changing $f(M, t)$ is insufficient here. Thus, for $U = c(M_1 + M_2)^2$ the computations were carried out with the stepsize $\Delta t = 2 \times 10^{-4}$ at $M_{\max} \approx 3 \times 10^2$ and $\Delta t = 1.5 \times 10^{-5}$ at $M_{\max} = 5 \times 10^3$ (mass given in units M_*, time in units $1/(cN_0M_*^2)$). In both cases Δt is much less than the time during which the distribution changes essentially (see figure 1(*b*)).

The explanation for this phenomenon is that the nonlinear set of differential equations, appearing after the integral in (I) is replaced by a sum, belongs to the so-called stiff sets (see for instance [12]). In such sets for stability one either has to choose a very small time stepsize or use special methods, stable for any Δt. In the former case the stiffer the system is the more CPU time is required. In the latter case the algorithm becomes much more complicated (in particular, due to the necessity of solving a set of nonlinear algebraic equations at each step), much more time is required to work out the program, CPU time increases compared with ordinary methods but it does not depend on the stiffness of the system. For very stiff systems (very large $M_{\max}$ in our case) the latter variant would be preferable. However, for the values of the parameters used in this article the former variant proved to be satisfactory.

The indicated instability for the Smoluchowski equation may be illustrated for the simplest method of solving differential equations—the Euler method, where

$$f(M, t + \Delta t) = f(M, t) + \dot{f}(M, t)\Delta t.$$

Let the error $\delta f(M, t)$ equal zero at all grid points M_j, except for some $j = i$, at some time t. Then it can be demonstrated (see appendix) that the error at the next step

$$\delta f(M_i, t + \Delta t) = -k\delta f(M_i, t)\Delta t$$

$$k = \frac{2cM^{\lambda}\mathcal{M}}{\Delta M} \qquad \text{for } U = c(M_1 + M_2)^{\lambda} \tag{4}$$

$$k = \frac{2cM^{\lambda/2}}{\Delta M}\int_0^{\Delta M} fM^{1+(\lambda/2)}\,\mathrm{d}M \qquad \text{for } U = c(M_1M_2)^{\lambda/2}$$

for the solving method we used (ΔM is the mass stepsize, depending on M; M changes from 0 to $M_{\max}$). So for $\Delta t > (\Delta t)_{\text{stab}} = 2/k$ the error grows with time. The stability condition for the second-order Runge–Kutta method can be shown to be the same as that for the Euler method: $\Delta t < 2/k$. The required stepsize $(\Delta t)_{\text{stab}}$ decreases with increasing $M_{\max}$. Formula (4) is approximate: to find $(\Delta t)_{\text{stab}}$ exactly one should know the eigenvalues of the matrix on the right-hand side of the set after linearization [12]. So we determined the required stepsize experimentally.

3. Dependence on $M_{\max}$ and the limit of large $M_{\max}$

When solving the Smoluchowski equation numerically, we introduced a finite limit mass $M_{\max}$, up to which computations were executed. The integral from 0 to ∞ in (1) was replaced by an integral from 0 to $M_{\max}$. Physically this corresponds to a sink of particles at large masses.

At the beginning we consider the influence of the sink in the exactly solved case $U \propto M_1 M_2$ [1]. In this case at $M_{\max} \to \infty$ the distribution is known to tend to the solution of the Smoluchowski equation without the sink [1, 13]; this means that for large $M_{\max}$ the influence of the limit mass is small. The distribution function for $U = cM_1M_2$ and finite $M_{\max}$ can be written in the form

$$f_{M_{\max}}(M,t) = f_\infty(M,t) \exp\left(Mc \int_0^t \Delta\mathcal{M}(t')\,\mathrm{d}t'\right) \tag{5}$$

where $\Delta\mathcal{M}(t) = \mathcal{M}_\infty(t) - \mathcal{M}_{M_{\max}}(t) = \int_0^\infty M f_\infty \,\mathrm{d}M - \int_0^{M_{\max}} M f_{M_{\max}}\,\mathrm{d}M$ is the total mass difference without the sink and with it. Substituting (5) in the definition of $\Delta\mathcal{M}$ and knowing $f_\infty(M,t)$, one can obtain an equation for $\Delta\mathcal{M}(t)$. The result is that the exponent in (5) is small at $s(t) \ll M_{\max}$, $M \ll M_{\max}$ and of order of 1 when $s(t) \gtrsim M_{\max}$, $M \sim M_{\max}$ ($s(t) = \infty$ at $t \geqslant t_{\text{cr}}$). Thus, the influence of finite $M_{\max}$ on the solution of the Smoluchowski equation is the following: (i) the total mass begins to decrease somewhat earlier than at t_{cr}; (ii) there is a rise on the right-hand end of the distribution function at $M \sim M_{\max}$, $t \gtrsim t_{\text{cr}}$; (iii) the second moment remains large, but finite at $t \geqslant t_{\text{cr}}$. This influence tends to zero when $M_{\max} \to \infty$.

The numerical solution of the Smoluchowski equation demonstrates two cases. For $U \propto (M_1M_2)^{\lambda/2}$ at $0 \leqslant \lambda \leqslant 2$ and for $U \propto (M_1 + M_2)^\lambda$, $0 \leqslant \lambda \leqslant 1$ the influence of $M_{\max}$ qualitatively (and quantitatively at $U \propto M_1M_2$) is similar to the one described above. The situation for the kernel $U \propto (M_1 + M_2)^\lambda$ at large λ (close to 2) is different. The value of $M_{\max}$ essentially influences the behaviour of the distribution moments (figures 2 and 3). The distribution function differs from one for $\lambda < 1$: a slowly decreasing tail to the distribution is formed at a very small time (figure 1(*b*)).

According to analytical results [14], the Smoluchowski equation has no solutions for $\mu < \nu - 1$, $\lambda > 1$ (at $M_{\max} = \infty$). This means that the limit $M_{\max} \to \infty$ does not exist for the solution corresponding to $U \propto (M_1 + M_2)^\lambda$. The existence of finite $M_{\max}$ has physical meaning: coalescences may be described correctly by the Smoluchowski equation with a given kernel in a bounded mass range only [1, 15]. In the case when the problem with infinite $M_{\max}$ has no solutions, the physical limit mass must be taken into account in the formulation of the problem.

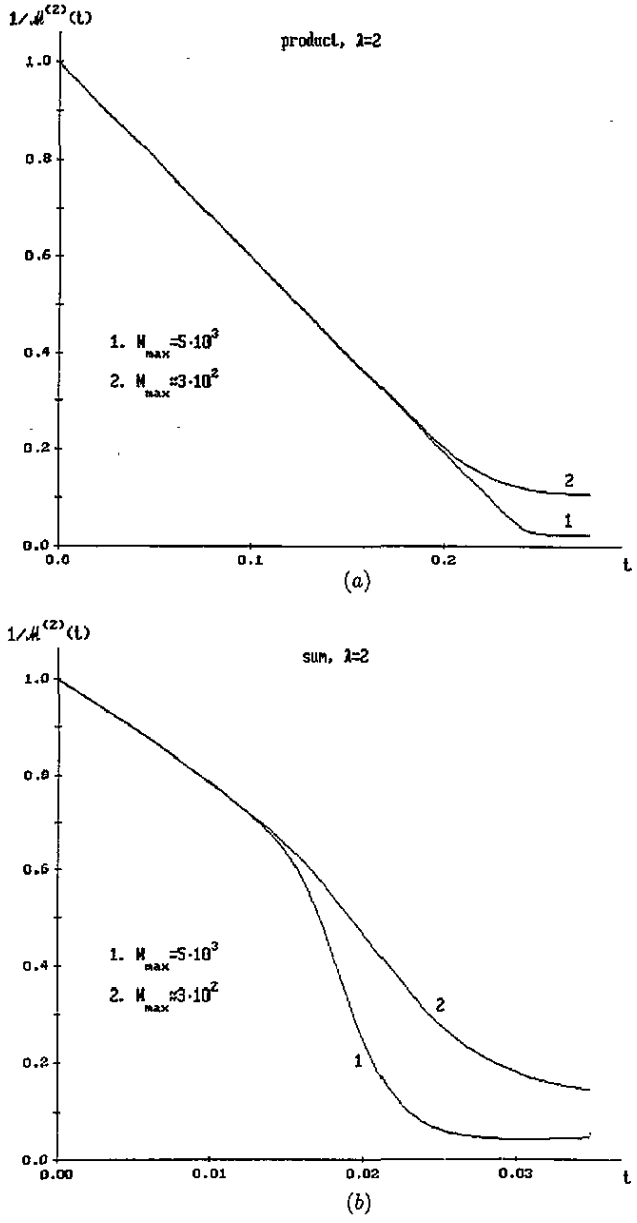

Figure 2. Behaviour of the second moment of the distribution $\mathcal{M}^{(2)}(t)$ (in units $\mathcal{M}^{(2)}(0)$) for (*a*) $U \propto M_1 M_2$ and (*b*) $U \propto (M_1 + M_2)^2$.

4. Self-similar behaviour of the distribution function

As known, in many cases the Smoluchowski equation has a self-similar solution

$$f(M,t) \propto s^{-\tau}(t)\varphi(M/s(t)) \tag{6}$$

where $\tau = 2$ for $\lambda \leqslant 1$ and $\tau > 2$ for $\lambda > 1$ (see [2, 7]). At the same time, it is not always known whether such a solution exists. Moreover, even if such a solution exists, the

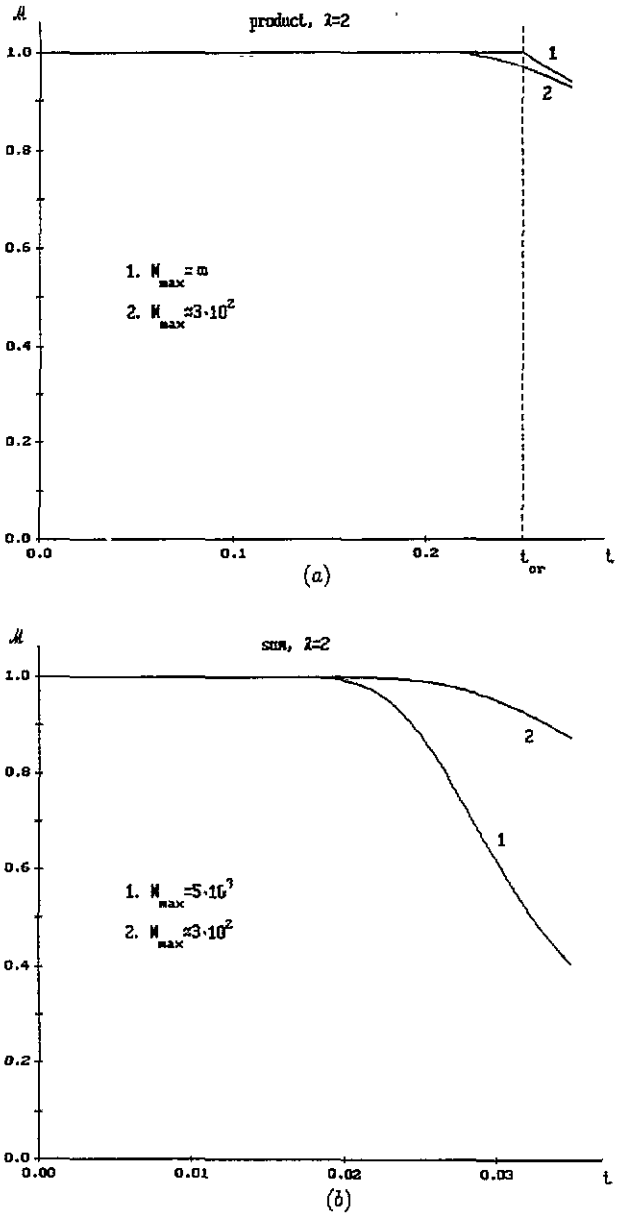

Figure 3. Behaviour of the total mass for (*a*) $U \propto M_1 M_2$ and (*b*) $U \propto (M_1 + M_2)^2$. In the case (*b*), unlike (*a*), the larger $M_{\max}$ the earlier the mass begins decreasing. This is related to strengthening of the influence of the sink with the increase in $M_{\max}$. The curve 1 in (*a*) is an exact analytical solution [1], the other curves are obtained numerically.

mass distribution will not necessarily tend to the scaling form after a transition period [2, 7]. Direct numerical solution of the Smoluchowski equation gives the possibility of determining whether the solution is self-similar.

The results for the kernels being considered here are the following. The solution for $U \propto (M_1 M_2)^{\lambda/2}$ tends to the self-similar one both at $0 < \lambda \leqslant 1$ and at $1 < \lambda \leqslant 2$. The solution for $U \propto (M_1 + M_2)^{\lambda}$, $0 < \lambda \leqslant 1$ is also self-similar, but for $\lambda > 1$ the situation is

different: the farther λ moves from 1, the greater the difference between the solution and the scaling form (6) becomes. For $\lambda \lesssim 1.3$ the solution still appears to be self-similar; for $\lambda \gtrsim 1.3$ this is not so. The non-scaling behaviour in this case seems to be related to the fact that the finiteness of the maximum mass essentially influences the solution (see section 3).

Figure 4 illustrates the approach of distribution to (6) in the course of time. The solution coincides with the scaling expression in the mass range $M \gg M_*$, this corresponds to the argument in (6) $x \gg (M_*/s(t))$. At $M \lesssim M_*$ the distribution retains information about the initial conditions. Hence, there are three mass regions: at $M \lesssim M_*$ the distribution depends on $f_0(M)$; at $M_* \ll M \ll s(t)$ the intermediate asymptotics are formed [16] (for $U \propto (M_1 + M_2)^\lambda$ these asymptotics are $M^{-\alpha}$) and at $M \gtrsim s(t)$ it decreases exponentially (see figure 1(*a*)).

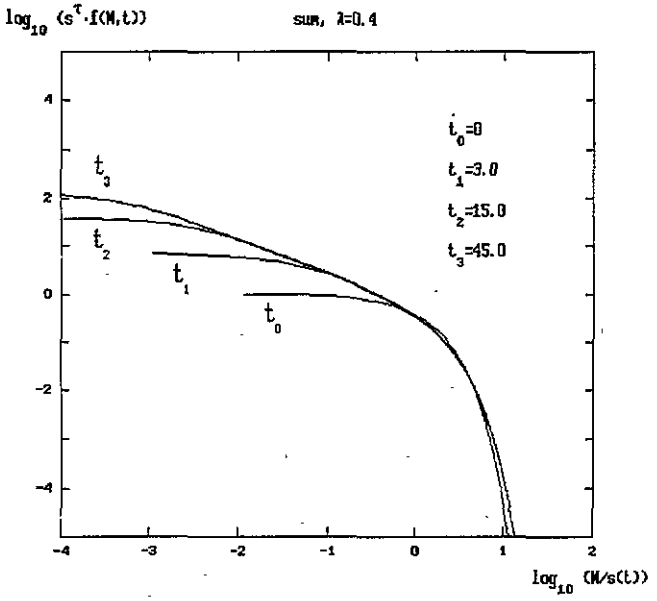

Figure 4. The approach of the distribution to the universal scaling form ($U = c(M_1 + M_2)^\lambda$, $\lambda = 0.4$). Beginning with t_1, the curves for different times almost coincide, except for small masses. The smaller M/s the longer the time before the solution becomes self-similar. (In this and the next figure $s(t)$ was determined from $\mathcal{M}^{(2)}(t)$. For $\tau = 2$, $\alpha < 2$ we have $s(t) \propto \mathcal{M}^{(2)}(t)$. However, for (9) this must fail at extremely large t because effective α becomes larger.)

The numerical solution allows us to obtain the scaling function $\varphi(x)$ in expression (6). For $U \propto (M_1 + M_2)^\lambda$, $\lambda \leqslant 1$ it can be approximated with high precision by the simple expression

$$\varphi(x) = Ax^{-\alpha}e^{-bx} \tag{7}$$

where A, b are constants. The formula (7) is analogous to the expression for φ in exactly solved cases and is similar to the Schechter function used to describe the galaxy mass distribution [17]. The values of the exponent α, as a function of λ, are given below in table 1. At very large x expression (7) has to fail because it does not coincide with the known analytical asymptotic behaviour [2,7]. For $U \propto (M_1 M_2)^{\lambda/2}$ the function φ has a more complicated form (see figure 5(*b*) below and figure 1(*c*)). As will be shown in section 5.1, its asymptotics at $x \to 0$ are non-power.

Table 1. Exponents of the intermediate asymptotics for $U \propto (M_1 + M_2)^{\lambda}$, $0 \leqslant \lambda \leqslant 1$.

λ	α
0.0	0.00
0.1	0.20
0.2	0.38
0.3	0.55
0.4	0.70
0.5	0.85
0.6	0.99
0.7	1.12
0.8	1.25
0.9	1.37
1.0	1.50

5. Asymptotics, exponents and t_{cr}

As known, the self-similar solution (6) often has a power-law asymptotic behaviour

$$\varphi(x) \sim x^{-\alpha} \qquad x \to 0. \tag{8}$$

Then a wide region with $f(M,t) \propto M^{-\alpha}$, corresponding to $M_* \ll M \ll s(t)$, appears after some time [16]. The exponent α can be obtained analytically for certain kernels, but, in general, its determination requires numerical computation.

At $\lambda > 1$ a phase transition takes place in the system. The phase transition may be characterized by the critical time t_{cr} and the exponent τ in the expression (6) ($\tau = 2$ for $\lambda \leqslant 1$, $\tau = \alpha$ for $\lambda > 1$). Finding t_{cr} and τ also requires numerical computation in general.

In this section we present such numerical computations.

5.1. Intermediate asymptotics and a method for determining the exponent

To determine the exponent α in (8) we plotted the local value of the exponent $\mathrm{d}(\log_{10} f(M,t))/\mathrm{d}(\log_{10} M)$ as a function of M. The region of the power-law intermediate asymptotics $f \propto M^{-\alpha}$ corresponds to

$$\frac{\mathrm{d}(\log_{10} f)}{\mathrm{d}(\log_{10} M)} = \text{constant} = -\alpha.$$

The plot for $U \propto (M_1 + M_2)^{\lambda}$, $\lambda = 0.4$ is shown in figure 5(*a*). One can see that the region with $\alpha \approx 0.70$ does form after some time. The rise at small masses is associated with the influence of the initial distribution at $M \lesssim M_*$; the fall at large ones is associated with $M \gtrsim s(t)$.

To test the precision of the described method we determined α for the two exactly solved cases: $U \propto (M_1 + M_2)$ and $U \propto M_1 M_2$. The obtained α coincided with the exact values 1.5 and 2.5 respectively.

For $U \propto (M_1 M_2)^{\lambda/2}$ the asymptotics proved to be non-power law. Figure 5(*b*) shows that the local exponent $\mathrm{d}(\log_{10} f)/\mathrm{d}(\log_{10} M)$ does not tend to a constant at $x \to 0$. The plot at $M_*/s(t) \ll M/s(t) \ll 1$ is close to a straight line; therefore $\varphi(x)$ in this interval may be approximated as

$$\varphi(x) \sim x^{a \ln x + b}. \tag{9}$$

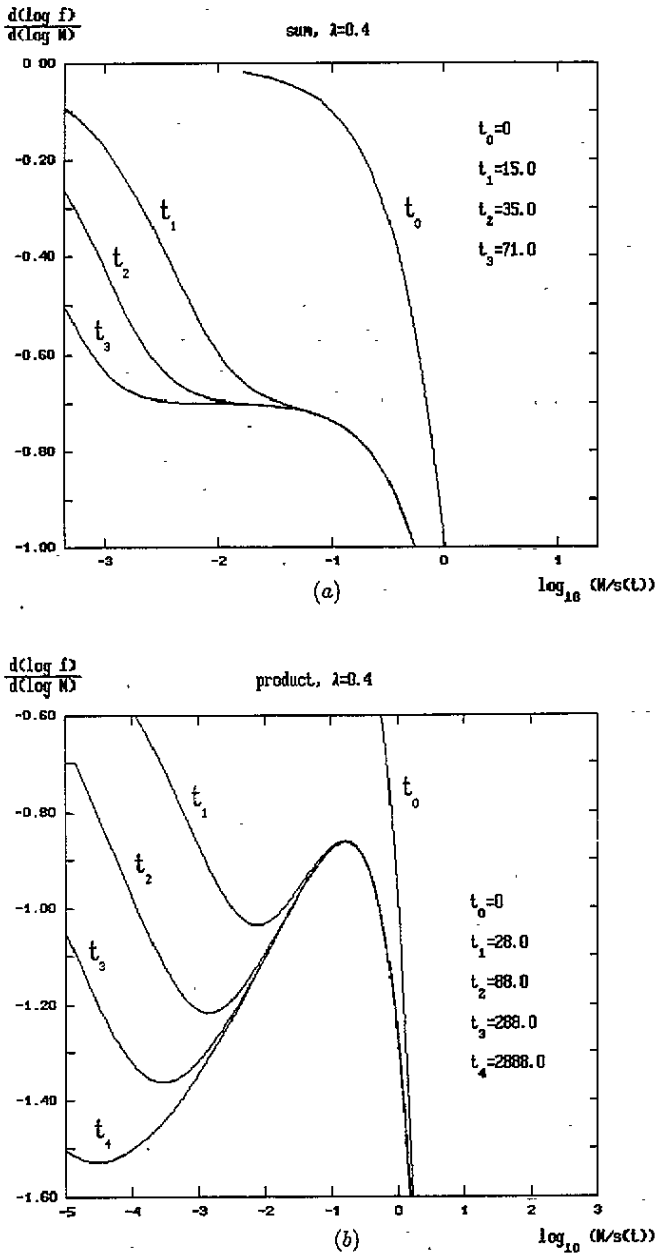

Figure 5. (*a*) The local value of the index $\mathrm{d}(\log_{10} f)/\mathrm{d}(\log_{10} M)$ for the kernel $U = c(M_1 + M_2)^{\lambda}$, $\lambda = 0.4$. A constant index region, corresponding to $f \propto M^{-\alpha}$, is formed with time (the part between x-coordinates -3 and -0.7). As t increases so does the region where the curve coincides with the universal function $\mathrm{d}(\log_{10} \varphi(x))/\mathrm{d}(\log_{10} x)$. (*b*) The same for $U = c(M_1 M_2)^{\lambda/2}$. The plot approaches a certain universal function with time (this testify to self-similarity), but the asymptotics of this function at $M/s \to 0$ are not the constasnt $-\alpha = -(\lambda + 1)$. Therefore, the asymptotics of $\varphi(x)$ at $x \to 0$ are non-power. The asymptotical region in the figure is close to a straight line—this corresponds to $\varphi(x) \approx x^{a \ln x + b}$ (the part between x-coordinates -4 and -1).

Hence the obtained solution does not agree with the known analytical one with the asymptotic behaviour

$$\varphi(x) \sim x^{-\alpha} \qquad x \to 0,\ \alpha = \lambda + 1.$$

Note that a self-similar solution with asymptotics like expression (9) cannot be obtained from the integro-differential equation for $\varphi(x)$ [1, 2, 7] because the integrals in this equation diverge. In this case for analytical investigation of the self-similar solution it is necessary to take into account explicitly the fact that the solution has the scaling form only at large enough M.

The result for $U \propto (M_1 M_2)^{\lambda/2}$, $0 < \lambda < 1$ is of great interest. At first sight, it seems to be in contradiction with known facts. As a matter of fact, however, it is not so. At first, the existence of a scaling solution with asymptotics $x^{-\lambda-1}$ has not been proved. Attempts to obtain the first correction to $x^{-\lambda-1}$ failed, and van Dongen and Ernst wrote in [7] (p 323), that they 'cannot exclude the possibility that in this case no solution $\varphi(x)\ldots$ exists that satisfies the physical requirement that the total mass be finite'. Second, disagreement with $x^{-\lambda-1}$ was already known [18], but it was earlier interpreted as a transitional region. Third, figure 1(*c*) shows the slope of $f(M)$ at constant M to change with time. It coincides with the result of [19]. Fourth, detailed information about the intermediate asymptotics cannot be obtained from the plot for $f(M)$ (figure 1). One can obtain this information by the method used in this article, that is from the plot of the local slope (figure 5).

5.2. The method for determining the critical exponents and t_{cr}

As mentioned above, the total mass $\mathcal{M}(t)$ starts to decrease when $s(t)$ becomes of order M_{max}. Therefore the phase transition time t_{cr} in numerical computations cannot be determined as the time when the mass ceases to be constant (at large times it is not conserved even for $\lambda \leqslant 1$). Neither can it be determined as the time when the second moment of the distribution $\mathcal{M}^{(2)}$ becomes infinite because, for finite M_{max}, all moments are finite and, at $s(t) > M_{max}$, $\mathcal{M}^{(2)}$ is almost constant.

In the present paper, t_{cr} was determined by extrapolation of the dependence of the second moment (pth moment $\mathcal{M}^{(p)}(t)$ in a more general case). This method may be illustrated by the example $U \propto M_1 M_2$ (figure 2(*a*)): extending the straight line until intersection with the axis of abscissa, one can find $t_{cr} = 0.25$.

The behaviour of $s(t)$ and $\mathcal{M}^{(p)}(t)$ at $t \to t_{cr}$ may be derived from the differential equation for $s(t)$, obtained by substitution (6) to (1)

$$\dot{s}(t) \propto s^{\lambda+2-\tau}$$

$$s(t) \propto (t_{cr} - t)^{-1/(\lambda+1-\tau)}.$$

Then we have

$$\mathcal{M}^{(p)} \propto (t_{cr} - t)^{-(p+1-\tau)/(\lambda+1-\tau)} \qquad (p > \tau - 1) \tag{10}$$

from the definition of $\mathcal{M}^{(p)}$ and expression (6). Thus we can find both t_{cr} and τ from the dependence $\mathcal{M}^{(p)}(t)$ at t close to t_{cr} (for $p \neq \lambda$). The results for τ should be compared with the theoretical prediction $\frac{1}{2}(\lambda + 3)$.

The procedure for determination of τ and t_{cr} was as follows. For every moment t_i we found three unknown parameters $A^{(local)}$, $t_{cr}^{(local)}$, $\tau^{(local)}$ in the formula $\mathcal{M}^{(p)} = A(t_{cr} - t)^{-(p+1-\tau)/(\lambda+1-\tau)}$ using three points t_{i-1}, t_i, t_{i+1}. Then $\tau^{(local)}(t)$ and $t_{cr}^{(local)}(t)$ were plotted. Extrapolation to the critical point gave the values of t_{cr} and τ.

The method was tested on the exactly solved case $U \propto M_1 M_2$ and the partly solved case $U \propto M_1^{\lambda} M_2^{\lambda}/[(M_1 + M_2)^{\lambda} - M_1^{\lambda} - M_2^{\lambda}]$ [2] for which t_{cr} is known. The obtained values are in agreement with the known analytical ones.

5.3. The results for exponents and t_{cr}

Values of the exponents of the power-law asymptotics α for $U \propto (M_1 + M_2)^\lambda$, $0 \leqslant \lambda \leqslant 1$ are presented in table 1. The limiting cases $\alpha = 0$, $\alpha = 1.5$ at $\lambda = 0$ and $\lambda = 1$ respectively coincide with the known exact solutions of the Smoluchowski equation. The function $\alpha(\lambda)$ is continuous at $0 \leqslant \lambda \leqslant 1$. Scaling theory [2, 7] does not give an explicit prediction for α in this case, but gives some restrictions [20]. The obtained values of α satisfy the restrictions.

The intermediate asymptotics of $f(M, t)$ for $U \propto (M_1 + M_2)^\lambda$, $1 < \lambda \leqslant 2$, may be non-power: the region with a constant value of the function $\mathrm{d}(\log_{10} f)/\mathrm{d}(\log_{10} M)$ seems to be absent (especially at large λ, close to 2; see figure 1(*b*)).

In table 2 we present the indices $\tau(= \alpha)$ and the values of t_{cr} for $U \propto (M_1 M_2)^{\lambda/2}$ at $\lambda > 1$, found from the behaviour of moments $\mathcal{M}^{(p)}(t)$ near t_{cr}. The obtained values of τ are close to $\frac{1}{2}(\lambda + 3)$, predicted analytically, but do not coincide with it. The difference between τ and $\frac{1}{2}(\lambda + 3)$ does not decrease with decrease in time or mass stepsize, or increasing M_{max}. Therefore this difference does not seem to be related to an error in the computation of $f(M, t)$. However, one cannot eliminate the possibility that this discrepancy may be explained by the difference between the exact time dependence of $\mathcal{M}^{(p)}$ and the asymptotic formula (10).

Table 2. Critical exponents and t_{cr} for $U = c(M_1 M_2)^{\lambda/2}$, $1 < \lambda \leqslant 2$. Critical time given for (2) in units $1/(cN_0 M_*^\lambda)$ (see also the second part of the footnote on p 000).

λ	t_{cr}	τ	$\frac{1}{2}(\lambda + 3)$
1.1	10	2.05	2.05
1.2	4.0	2.08	2.10
1.3	2.2	2.10	2.15
1.4	1.4	2.15	2.20
1.5	1.01	2.19	2.25
1.6	0.74	2.23	2.30
1.7	0.55	2.30	2.35
1.8	0.42	2.38	2.40
1.9	0.32	2.44	2.45
2.0	0.25	2.50	2.50

6. Conclusions

Numerical solution of the Smoluchowski kinetic equation using the methods described here allows us to find the mass distribution function in a wide range of masses; to determine whether the solution is self-similar; to obtain the scaling function; and to find the exponent in case of power-law asymptotics. For $\lambda > 1$ it is possible to find the critical exponents and t_{cr} from the behaviour of moments, on the condition that the solution is self-similar.

The results for the kernels considered are the following. For $U \propto (M_1 + M_2)^\lambda$, $\lambda \leqslant 1$ *the solution is self-similar (asymptotically); the scaling function is close to the simple* expression (7); the intermediate asymptotics at $M_* \ll M \ll s(t)$ are power law with the exponents given in table 1. For $U \propto (M_1 + M_2)^\lambda$, $\lambda > 1$ the farther λ is from 1, the greater the difference between the self-similar behaviour and the distribution becomes and the more dependent $f(M, t)$ becomes on the value of M_{max}. For $U \propto (M_1 M_2)^{\lambda/2}$, $0 < \lambda \leqslant 2$ the

solution is self-similar. The critical exponents and t_{cr} for $\lambda > 1$ are given in table 2. The intermediate asymptotics for $\lambda < 1$ proved to be non-power and to differ from the solution known earlier. Some features of the numerical solutions obtained are also discussed in [21]. Note also that the properties of the solution of the Smoluchowski equation are very close to those of the kinetic equations which appear in the weak turbulence theory (see, e.g., [22], p 200).

Acknowledgments

I thank V M Kontorovich and A V Kats for ve· ·lpful discussions of the work. The work was supported in part by the Ukrainian St mittee for Science and Technology (theme 'Quasar').

Appendix

Here we derive formula (4). For definiteness, me $U(M_1, M_2) = c(M_1 + M_2)^\lambda$. Let the error in the distribution function $\delta f(M, t)$ time be different from 0 in only one grid point M_j (we shall assume that the ma large, close to M_{max}). Then the error at the next step can be obtained from (1):

$$\delta f(M_j, t + \Delta t) \approx 2cM_j^\lambda \int_0^{M_j/2} f(M') \,\mathrm{d}M' - 2c\delta f(M_j) \times \int_0^\infty (M_j + M')^\lambda f(M \quad f(M_j) \int_0^\infty (M_j + M')^\lambda \delta f(M') \,\mathrm{d}M'. \tag{11}$$

The function f (and the in (1) is calculated by t used, we may assume δf ıe grid points only. Since the integral to obtain $f(M_j - M_i)$ interpolation is

$$\delta f(M) \approx \begin{cases} \delta f(M_j \cdot & M_{j-1} \leqslant M \leqslant M_{j+1} \\ 0 & \text{otherwise} \end{cases}$$

where ΔM_j is the mass stepsize (at the point M_j). Then (11) leads to

$$\delta f(M_j, t + \Delta t) \approx 2cM_j^\lambda \delta f(M_j, t) \int_0^{\Delta M_j} f(M') \left(1 - \frac{M'}{\Delta M_j}\right) \mathrm{d}M' - 2cM_j^\lambda \delta f(M_j, t) \times \int_0^\infty \left(1 + \frac{M'}{M_j}\right)^\lambda f(M') \,\mathrm{d}M' - 2cf(M_j) \int_0^\infty (M_j + M')^\lambda \delta f(M') \,\mathrm{d}M'. \tag{12}$$

Since the stepsize ΔM increases with mass (see section 2.1), at large M_j, the inequality

$$M_j \gg \Delta M_j \gg M_*$$

is realized and the integral from 0 to ΔM in (12) may be replaced by the integral from 0 to ∞. After this (12) may be written in the form

$$\delta f(M_j, t+\Delta t) \approx -2cM_j^{\lambda}\frac{\mathcal{M}}{\Delta M_j}\delta f(M_j,t) - 2cf(M_j)\int_0^{\infty}(M_j+M')^{\lambda}\delta f(M')\,\mathrm{d}M'. \qquad (13)$$

The value of $f(M_j)$ is very small at large M_j (see, e.g., figure 1(b)), so we can neglect the second term in (13). Then

$$\delta f(M_j, t+\Delta t) \approx -k\delta f(M_j,t)$$

$$k = 2cM_j^{\lambda}\mathcal{M}/\Delta M_j.$$

The analogous derivation for $U = c(M_1M_2)^{\lambda/2}$ results in the formula

$$k = \frac{2cM_j^{\lambda/2}}{\Delta M_j}\int_0^{\Delta M_j} f(M)M^{1+\lambda/2}\,\mathrm{d}M.$$

References

[1] Voloshchuk V M 1984 *Kinetic Theory of Coagulation* (Leningrad: Gidrometeoizdat)
[2] Ernst M H 1986 *Proc. Sixth Trieste Int. Symp. on Fractals in Physics (Trieste, 1985)* ed L Pietronero and E Tosatti (Amsterdam: North-Holland)
[3] Kats A V and Kontorovich V M 1990 *Zh. Exp. Teor. Fiz.* **97** 3 (*Sov. Phys.–JETP* **70** 1)
[4] Cavaliere A, Colofrancesco S and Menci N 1992 *Astrophys. J.* **392** 41
[5] Kontorovich V M, Kats A V and Krivitskiĭ D S 1992 *Pis'ma Zh. Exp. Teor. Fiz.* **55** 3 (*Sov. Phys.–JETP Lett.* **55** 1)
[6] Kats A V and Kontorivich V M 1991 *Pis'ma Astron. Zh.* **17** 229 (*Sov. Astron. Lett.* **17** 96)
[7] Van Dongen P G J and Ernst M H 1988 *J. Stat. Phys.* **50** 295
[8] Stockmayer W H 1943 *J. Chem. Phys.* **11** 45
[9] Trubnikov B A 1971 *Dokl. Akad. Nauk SSSR* **196** 1316 (*Sov. Phys.–Dokl.* **16** 124)
[10] Hausman M A and Ostriker J P 1978 *Astrophys. J.* **224** 320
[11] Voloshchuk V M and Sedunov Yu S 1975 *Processes of Coagulation in Disperse Systems* (Leningrad: Gidrometeoizdat)
[12] Rakitsky Yu V, Ustinov S M and Chernorutsky I G 1979 *Numerical Methods for the Solution of the Stiff Differential Equations* (Moscow: Nauka)
[13] Bak Thor A and Heilmann Ole 1991 *J. Phys. A: Math. Gen.* **24** 4889
[14] Van Dongen P G J 1987 *J. Phys. A: Math. Gen.* **20** 1889
[15] Kats A V, Kontorovich V M and Krivitsky D S 1993 *Multi-wavelength Continuum Emission of AGN (Proc. IAU Symp. 159)* ed T J-L Courvoisier and A Blesha (Dordrecht: Kluwer) p 113
[16] Barenblatt G I 1982 *Similarity, Self-similarity and Intermediate Asymptotics* (Leningrad: Gidrometeoizdat)
[17] Schechter P 1976 *Astrophys. J.* **203** 297
[18] Gabellini Y and Meanier J L 1992 *J. Phys. A: Math. Gen.* **25** 3683
[19] Karg K, Redner S, Meakin P and Leyvraz F 1986 *Phys. Rev.* A **33** 1171
[20] Van Dongen P G J and Ernst M H 1985 *J. Phys. A: Math. Gen.* **18** 2779
[21] Kontorovich V M, Krivitsky D S and Kats A V 1995 *Physica* **D** in press
[22] Zakharov V E, L'vov V S and Falkovich G 1992 *Kolmogorov Spectra of Turbulence* (Heidelberg: Springer)